PERFORMANCE AND ANALYSIS OF ARTIFICIAL GROUND FREEZING IN THE SHIELD TUNNELING

Chang-Yu Ou[1], Chung-Cheng Kao[2], and Ching-I Chen[3]

ABSTRACT

To prevent any possible accident as shield machines enter into vertical shafts from soil or exit from soil into vertical shafts, artificial ground freezing is often conducted to form perfectly watertight between diaphragm walls and the adjacent soil. This paper presents the mechanical performance of the artificial ground freezing applied to shield tunneling in the construction of the Taipei MRT system. Two case histories at the same site, one with installation of vertical freezing tubes and the other with horizontal freezing tubes, are presented. Over the ground freezing period the temperature of the soil in the frozen region was monitored through the automatic data acquisition system to ensure the temperature of the destined soil matching the original design requirement, *i.e.*, below −1.0°C. Moreover, finite element analysis of temperature change over the period of ground freezing was carried out, in which the material parameters were determined with a reasonable procedure. Compared with the monitored results, the predicted values were in good agreement with the monitored ones. The numerical tool and procedure for determining material parameters are useful in predicting the temperature change during ground freezing.

Key words: Artificial ground freezing, shield tunneling, shafts, temperature change.

1. INTRODUCTION

With rapid growth of population in metropolitan areas, the demand for the mass rapid transit (MRT) system increases. Since the space for underground construction is usually limited, shield tunneling is often used for the construction of the MRT system. During the shield tunneling process, shield machines, placed in shafts, will be pushed into soil at the beginning of tunneling or pushed from soil into shafts at the end of tunneling. Such a process is the so-called mirror-face breaking.

Since the soil in the shaft is excavated, causing a large difference of the earth pressure below the excavation bottom in the shaft and that in the back of the diaphragm wall, the soil in the front of the diaphragm wall may collapse during the mirror-face breaking stage, along with the flowing water into the tunnel. Several case histories associated with accidents at the mirror-face breaking stage have been reported, for example, Fang *et al.* (2006), Yang and Chao (1997) and Ju *et al.* (1997). To ensure the safety at the stage of mirror-face breaking in shield tunneling, the soil in the region between diaphragm wall of vertical shafts and the adjacent soil should be perfectly watertight and with appropriate strength (Fig. 1). Jet grouting and artificial ground freezing (AGF) are two common methods used to strengthen the soil and to reduce the permeability of the soil in front of tunnels.

Artificial ground freezing involves the circulation of a refrigerated coolant through subsurface freezing tubes to extract heat until the temperature is below the freezing point. Within each freezing tube, a smaller diameter of tube is installed

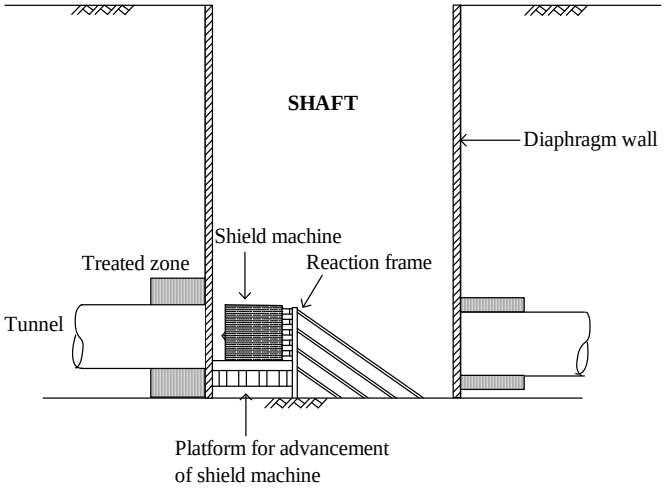

Fig. 1 Schematic diagram for the treated region at the mirror face

permitting the downward circulation of the coolant which then flows to the surface through the annulus of the larger tube. The soil water is then frozen and become a strong and watertight material. The material is so strong that it is routinely used as groundwater control and soil support for the construction of shafts. Compared with the jet grouting, the artificial ground freezing is a relatively stable and effective method for groundwater control and soil strengthening but costly (Whittaker and Frith, 1990).

Artificial ground freezing techniques have been applied to groundwater control and soil support, *e.g.*, Clarke and MacKenzie (1994), Zhou *et al.* (1999), Yu *et al.* (2005) and Crippa and Manassero (2006). Several researchers have conducted theoretical work of ground freezing or heat transfer problems in geomaterial. For example, Yang and Pi (2001), Lackner, *et al.* (2005), Lai *et al.* (2005), and Li *et al.* (2006). With artificial ground freezing, practical engineers should clearly know how

Manuscript received February 9, 2009; revised April 17, 2009; accepted April 17, 2009.

[1] Professor (corresponding author), Department of Construction Engineering, National Taiwan University of Science and Technology, Taipei City 10607, Taiwan, ROC.

[2] Deputy Director General, Department of Rapid Transit Systems, Taipei City Government, Taipei City 10448, Taiwan, ROC.

[3] Graduate student, Department of Construction Engineering, National Taiwan University of Science and Technology, Taipei City 10607, Taiwan, ROC.

long is needed to achieve the minimum thickness of ice wall. It can be done with theoretical analysis, past experiences or numerical analysis. Since the quantity, spacing, depth and size of the freezing tubes are unique to each site, theoretical analysis and past experiences sometimes have limitations. Hence numerical analysis, along with calibration of parameters, is preferably performed to obtain an accurate prediction.

This paper presents the performance of artificial ground freezing applied to the shield tunneling, in which the interface between shaft and adjacent soils was frozen. The case histories were well monitored in temperature field. Numerical analysis is then performed to validate the analysis procedure established in this paper.

2. DAOCHA SECTION OF THE TAIPEI MRT LINE

The Daocha section was the junction of the Xinzhuang line and Luzhou line of the Taipei MRT system. As shown in Fig. 2, the section is with 125 m long and 15 m wide in the eastern side and 26 m wide in average in the western side. The section, located below the Danshui river (Figs. 2 and 3), was constructed with the cut and cover method, in which the final excavation depth was near 40 m below ground surface and a 2.0 m thick diaphragm wall and temporary steel struts were used as the earth retaining structure.

Generally, the Taipei basin is formed by a thick alluvium formation, *i.e.*, Sungshan Formation, which lies above a gravel formation. The subsurface condition is consisted of soft clay layers and sand layers, which appear alternately. The groundwater level at the excavation site was at GL–3.3 m (GL refers to the ground surface level). The porewater pressure in this region is generally recognized as the hydrostatic condition. Typical soil properties of the alluvium formation have been discussed by many investigators, *e.g.*, Huang *et al.* (1987) and Woo and Moh (1990).

2.1 Performance of the Ground Freezing at the Construction Site W1

In the western side of the section, dubbed as the construction site W1, the excavation went as deep as 39.81 m. A shield machine was pushed from the section, *i.e.*, vertical shaft, into soil for tunneling process. Table 1 lists the basic soil properties of the soil at the site.

During the mirror-face breaking stage, any leakage of groundwater into the freezing area will cause loosening of the surrounding soil, which in turn brings the water in the Danshui river flowing into the whole tunnel. The tunnel may thus collapse totally. For doubly securing the tunnel, prior to artificial ground freezing, jet grouting was executed first in the zone of 4.6 m from the diaphragm wall and between the depth of 18 m and 39.81 m. According to test data, the average void ratio and water content for the treated soil were 0.62 and 52.2%, respectively.

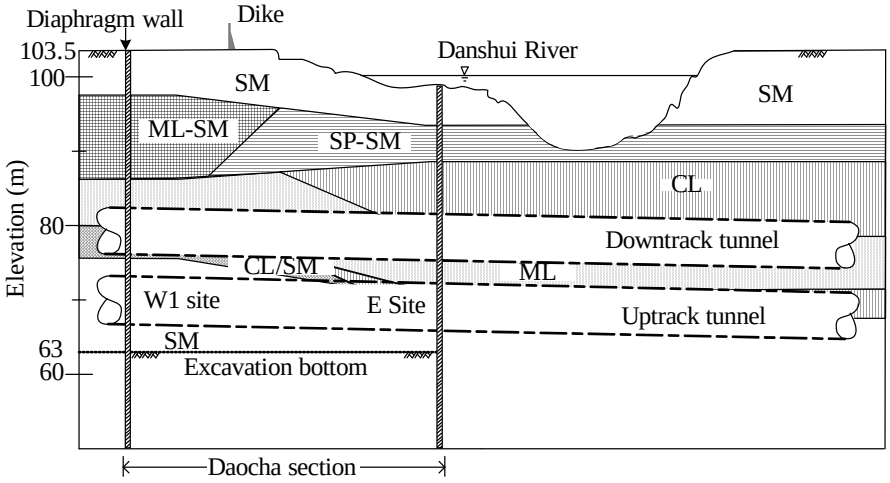

Fig. 2 Geological profile and tunnels of the Daocha section

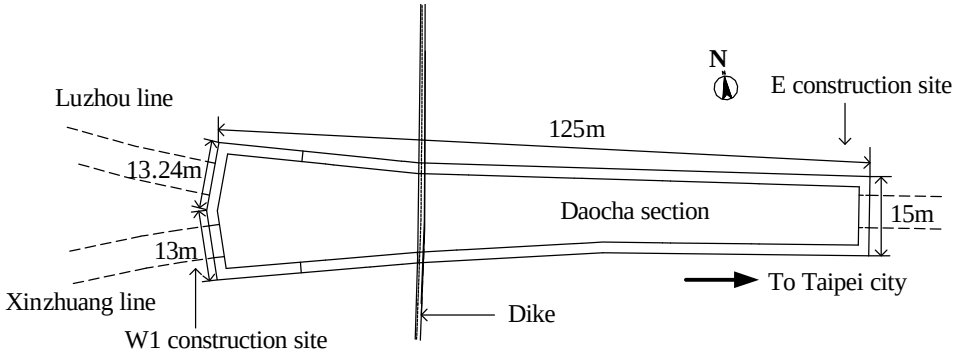

Fig. 3 Plan of the Daocha section

Table 1 Basic soil properties at the construction site W1

Type of soil	Depth (m)	γ_t (kN/m^3)	ω (%)	*e*	SPT-N
SM	–2.2	20.4	18.20	0.54	7
SM	–6	18.0	21.03	0.72	9
ML/SM	–17.2	19.7	25.20	0.71	9
ML	–23.7	19.6	24.50	0.71	10
CL/SM	–28	19.7	24.70	0.70	13
SM	–33.6	20.4	20.40	0.58	24
SM	–36.2	20.6	17.40	0.51	12
SM	–42.5	19.9	24.30	0.66	30
GP	–70	21.0	20.00	0.60	> 100

γ_t : unit weight of soil, ω: gravitational water content, *e*: void ratio

Vertical freezing tubes were installed in two rows with a spacing of 0.7 m (Fig. 4). The first row (V01 to V15) were 0.5 m from the diaphragm wall, with a spacing of 0.8 m between freeze tubes while the second row (V16 to V23) 1.2 m from the diaphragm wall, with a spacing of 1.6 m between freezing tubes. The frozen region was confined between GL–27.47 m and GL–39.47 m. A total of five temperature measurement tubes (VT1 to VT5) were installed, of which VT1 and VT2, near the edge of the tunnel, were 1.0 m from the diaphragm wall, VT3 and VT4, also near the edge, were 1.8 m from the diaphragm wall, and VT5, near the center of the tunnel, was 1.5 m from the diaphragm wall. As shown in Fig. 5, fourteen sensors were installed in each tube. For assurance of the safety of tunnel, the sensors were placed with an interval of 2.0 m in depth in the zone of tunnel.

The freezing tubes and temperature measurement tubes are made of seamless steel tube, with an outer diameter of 114 mm and inner diameter of 102 mm. Outside the target frozen zone of the tube, PE (Polystyrene) was used as heat isolation material. Before the operation of ground freezing, the tubes were examined with the 700 kN/m^2 air pressure to ensure the tubes to be gastight. Brine was used as the coolant in this project. Over the period of ground freezing, the flow rate of the coolant in the circulation tubes was between 1500 L/min and 1600 L/min. The temperature of the coolant flowing into the tubes was controlled at −32.0°C while the temperature for the coolant flowing out of the tubes was around –29.9°C.

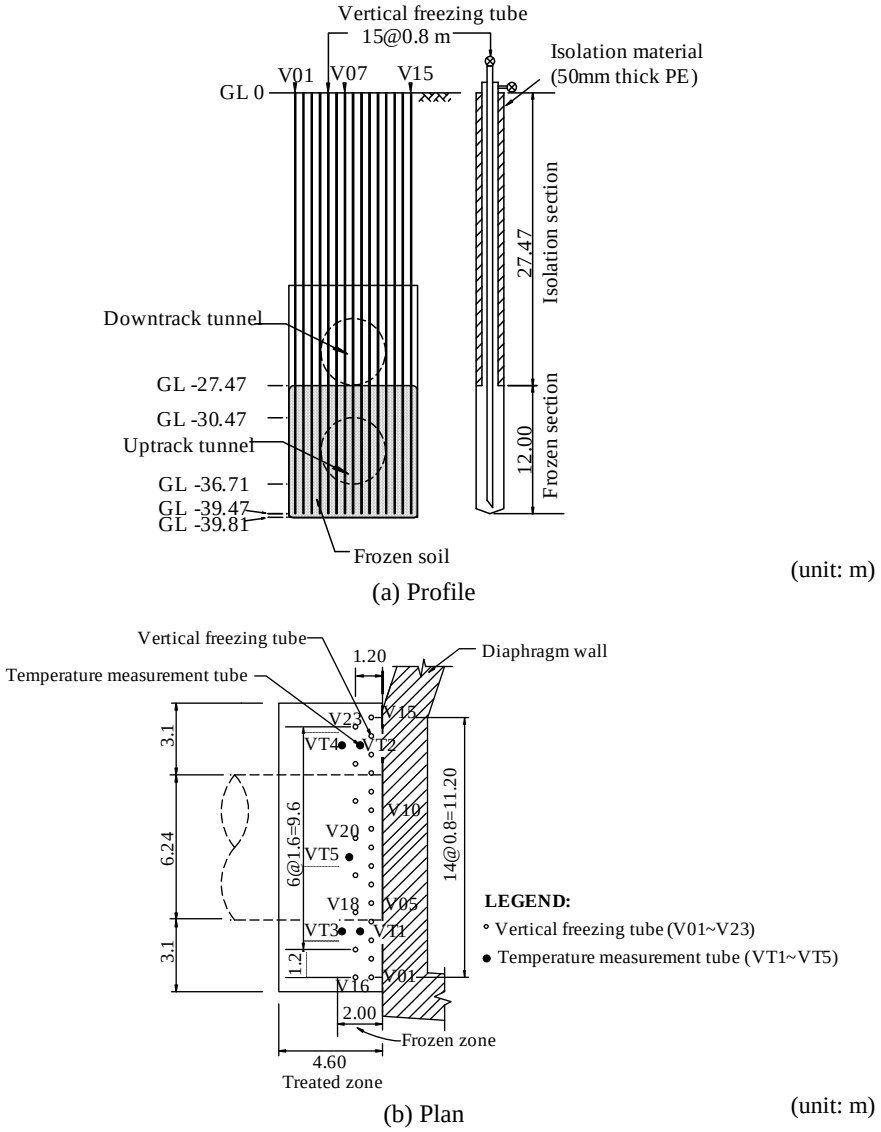

Fig. 4 Freezing tubes and temperature measurement tubes at the construction site W1

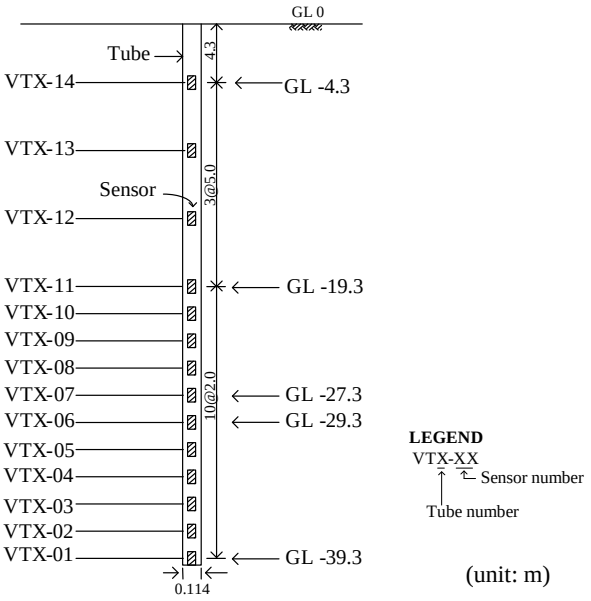

Fig. 5 Temperature measurement tube and depth of sensors at the construction site W1

The artificial ground freezing operated roughly 185 days, starting from the 15th of May 2006 to mirror-face breaking stage The mirror-face breaking process was completed in two stages. When the ice wall was formed to reach the 1.6 m thick, hydraulic breakers were used to the shatter the 1.9 m thick diaphragm wall. As the ice wall achieved 2.0 m thick, the rest of the 0.1 m thick diaphragm wall was cleared manually. After completion of the mirror-face breaking, the freezing tubes were lifted to the zone of down track tunnel, which was about 3.0 m above the up-track tunnel. Since the data from the down-track tunnel are not available, only the up-track tunnel data was used in this study.

Figure 6 displays the variation of temperature with time over the period of ground freezing. According to the figure, the temperature of the soil between GL–29.3 m and GL–39.3 m, *i.e.*, 10 m depth, fell below –1.0°C after 63 days (17th of July 2006) of the operation of ground freezing. Since the temperature measurement tubes, VT3 and VT4, were in a distance of 0.6 m from the second row of the freezing tubes, which were in turns 1.2 m from the wall, the frozen soil should at least achieve more than 1.8 m thickness behind the wall. Moreover, VT3 and VT4 were separated 8 m each other. We therefore infer that at this stage, the soil of 10 m deep, 8 m wide and 1.8 m thick was frozen.

We can also view from the figure that at the 85th day (8th of August 2006) of operation of ground freezing, the temperature of sensor VT1-07 and VT2-07 (GL–27.3 m) fell to below freezing point while sensors VT3-07, VT4-07 and VT5-07 were still unable to reach the freezing point. It was inferred that though the frozen soil was extended to GL–27.3 m, the frozen soil 3.17 m higher than crown of the up-track tunnel, the thickness of frozen soil at this level might not reach 2.0 m, as required by design. The freezing process certainly needed to be continued.

As shown in the figure, at the 147th day (9th of October 2006), all of the temperature measurement sensors, VT1-07 to VT5-07, fell to below the freezing point. The extent of the frozen soil should be at least 2.0 m thick above the crown, 8 m wide and 12 m deep, which is suitable for mirror-face breaking.

Figure 6 also shows that the temperature of the soil in the frozen zone but near its boundary was higher than those at the middle. Take an example of measurement of VT4-01 and VT4-06, which located near the boundary of frozen zone and were with the largest difference with those near the middle, for example, VT1-03 (Note: VT1-07 was outside the frozen zone). The temperatures of VT4-01, VT4-06 and VT1-03 at day 147 were equal to –5.5°C, –7.3°C and –16.0°C, respectively. The percentages of variation of measurement at VT4-01 and VT4-06

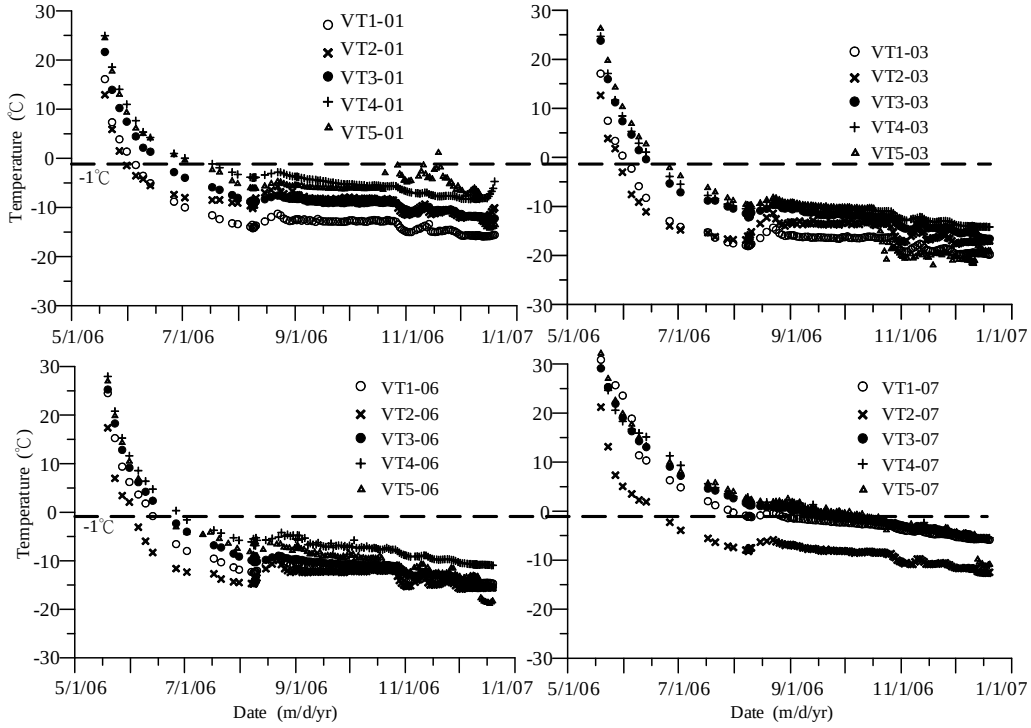

Fig. 6 Variation of temperature with time at the construction site W1

are 65% and 54%, respectively, compared with that at VT1-03. Such difference was acceptable and reasonable because ground freezing should have less effect on the soil near the boundary of the target frozen zone.

2.2 Performance of the Ground Freezing at the Construction Site E

In the eastern side of the section, dubbed as the construction site E, a shield machine was pushed from the soil into the shaft. The shaft was excavated to 39.7 m below the ground surface. Table 2 lists the basic soil properties at the site.

For doubly guarding the tunnel during the process of mirror-face breaking, jet grouting was first conducted at a depth of 18.55 m and 42.99 m below the ground surface, and within the zone of 6.63 m from the diaphragm wall. According to test data, the average void ratio and water content for the treated soil were 0.61 and 20.6%, respectively.

Then, thirty horizontal freezing tubes, with a length of 6.5 m for each tube, were installed at a distance of 3.62 m from the center of the tunnel (Fig. 7). Seven temperature measurement tubes, with a distance of 4.22 m away from the tunnel center and 0.6 m from the freezing tubes, were allocated surrounding the tunnel. As shown in Fig. 8, each tube contains seven sensors.

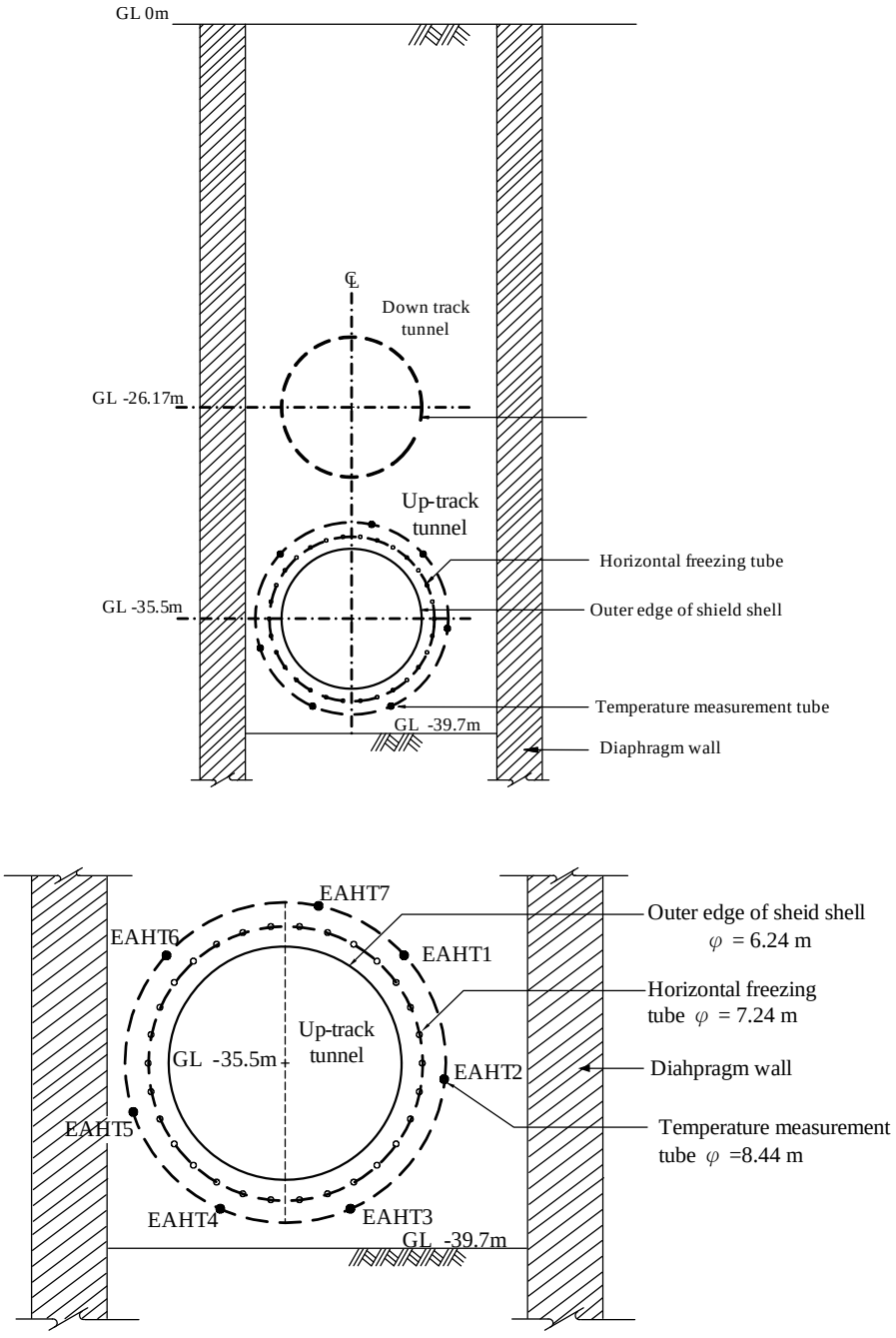

Fig. 7 Location of freezing tubes and temperature measurement tubes at the construction site E

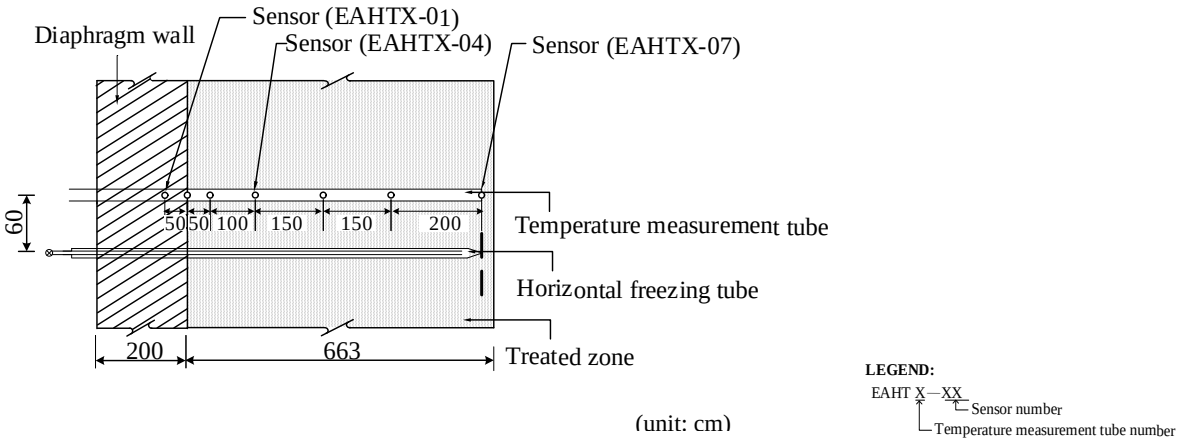

Fig. 8 Temperature measurement tube and location of sensors at the construction site E

Table 2 Basic soil properties at the construction site E

Type of soil	Depth (m)	γ_t (kN/m^3)	ω (%)	*e*	SPT-N
SF	–8	18.0	33.38	1.11	8
CL	–10	18.0	21.50	0.65	2
SP-SM	–15	19.4	33.33	1.03	13
CL	–25	19.3	33.17	0.97	8
ML	–32	19.5	27.82	0.76	13
CL	–36	19.8	25.80	0.76	12
SM	–43	20.0	25.20	0.74	27
SM	–58.3	19.9	18.98	0.63	33
GP	–70	21.0	20.00	0.60	> 100

Artificial ground freezing initiated at the 10th of November 2006. The mirror-face breaking stage was done at the 16th of January 2007. However, to maintain the stability of tunnel face and construction of the tunnel lining, the ground freezing was kept operation until the 1st of March 2007. The total freezing time was about 110 days. During freezing process, the flow rate of the coolant in the circulation tubes was between 1500 L/min and 1600 L/min. The temperature of the coolant flowing into the tubes was controlled at –30.0°C while the temperature for the coolant flowing out of the tubes was equal to –26.7°C.

Figure 9 displays the variation of temperature change with time for temperature measurement tubes, EAHT1, EAHT2, EAHT5, and EAHT7. Pattern of the monitoring results from the other temperature measurement sensors are similar to Fig. 9.

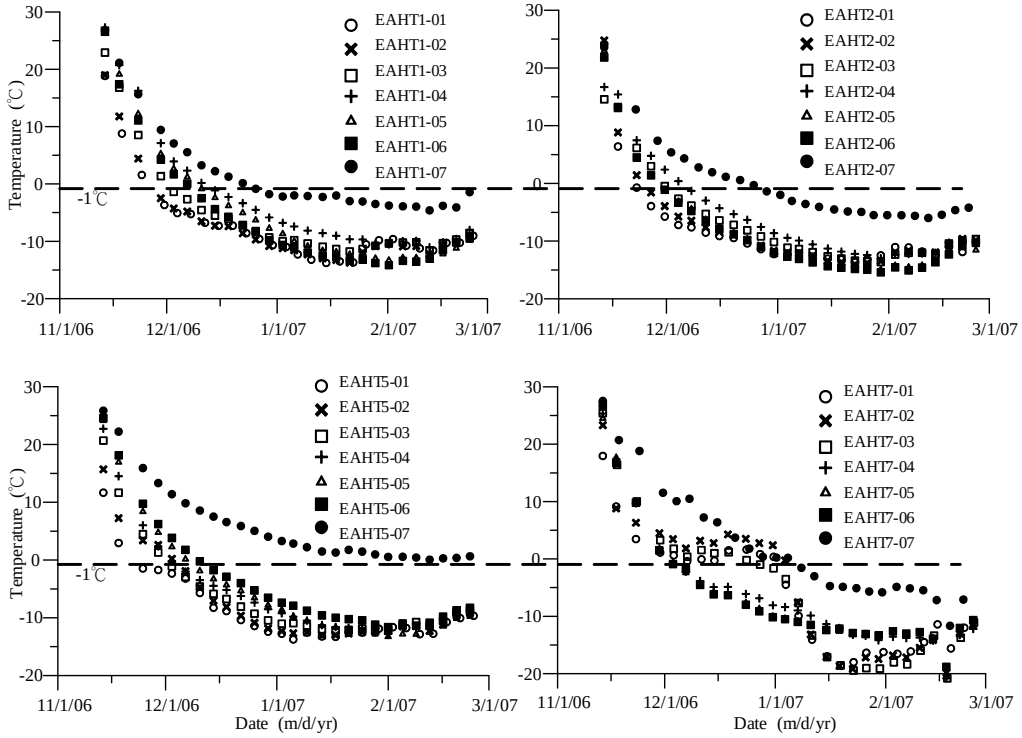

Fig. 9 Variation of temperature with time at the construction site E

According to the monitoring results, the ground freezing process seemed to have less effect on the soil near EAHT4 and EAHT5. At the 34th day (14th of December 2006) of ground freezing, some of the temperature measurement sensors, for example, EAHT1-01 to EAHT1-06 and EAHT2-01 to EAHT2-06 fell below −1.0°C. At the 54th day, only EAHT4-07 and EAHT5-07, 6.5 m from the diaphragm wall, were with the temperature higher than −1.0°C while all of the temperature measurement sensors, EAHTX-01 to EAHTX-06 (note: X = 1 to 6), fell below −1.0°C. Since the temperature measurement tubes were with 0.6 m from the freezing tube, the ring-like frozen soil would be around 1.2 m in thickness, which did not meet the original design thickness, *i.e.*, 1.6 m in thickness. The ground freezing was continued until the extent of frozen soil reached the designed range.

Figure 9 also shows that the sensors installed in the diaphragm wall, *e.g.*, EAHT-01, resulted in the lowest temperature measurement results because the thermal conductivity of the concrete was much larger than that of soil (Harris, 1995). Again, the temperature of the sensors near the boundary of the frozen zone, *e.g.*, EAHT1-06, was not much different with those in the middle.

Since only one row of freezing tubes was placed outside the tunnel, there were unable to know when the frozen soil reached the designed thickness. The numerical analysis was therefore carried out to predict the development of frozen soil during the operation of ground freezing, which will be discussed later in this paper.

3. FINITE ELEMENT ANALYSIS

In this study, a 2-D heat flow computer program TEMP/W (Krahn, 2004) is adopted for analysis, in which the following governing equation is used:

$$\frac{\partial}{\partial x}\left[k_x \frac{\partial T}{\partial x}\right]+\frac{\partial}{\partial y}\left[k_y \frac{\partial T}{\partial y}\right]+Q=\lambda \frac{\partial T}{\partial t} \tag{1}$$

where T is the temperature, k_x and k_y separately represent the thermal conductivity in the x and y directions, Q is the applied boundary flux, λ is the heat storage capacity, and t is time.

Therefore, the heat storage capacity (λ) and thermal conductivity (k) are required to solve the general heat problem. However, in soil, especially fine soils, some water is bound to the surface of the particles by means of chemical bonds and electrostatic forces. The binding forces are strongest at the particle surface and decreases with the distance from the particle surface to free water. Water in soil starts to freeze from which the binding forces are smallest, *i.e.*, free water and gradually expands to near the particle surface. Not all of the water in the soil experiences freezing at a single temperature. Therefore, heat storage capacity (λ) and thermal conductivity (k) of soil vary with the unfrozen water content, which in turns varies with the temperature (note: the unfrozen water content is the percentage of the water in soil that remains unfrozen at a certain temperature). The dependence of the unfrozen water content on temperature is thus required for analysis. In this study, the function of unfrozen water content to temperature as suggested by Willams (2001) is employed in the analysis.

According to the characteristics of heat storage, the heat storage capacity should be the sum of the volumetric heat capacity (C) of the material and the latent heat associated with the phase change, which can be expressed as

$$\lambda = C + L\frac{\partial w_u}{\partial T} \tag{2}$$

where C is the volumetric heat capacity, w_u denotes the unfrozen volumetric water content and L denotes the latent heat of water, which is equal to 3.34×10^5 kJ/m^3 (Harris, 1995; Krahn, 2004).

According to Johnston *et al.* (1981), the volumetric heat capacity, C, can be obtained by the following formula:

$$C = \gamma_d \left[c_s + c_w\, \omega_u + c_i\, \omega_f\right] \tag{3}$$

where γ_d is the dry unit weight of soil, c_s is the specific heat of soil, c_w is the specific heat of water, c_i is the specific heat of ice, ω_u is the unfrozen gravitational water content and ω_f is the frozen gravitational water content.

According to Harris (1995) and Krahn (2004), the values of c_s, c_w, and c_i can be set equal to 0.71, 4.187, and 2.094 kJ/kg-K, respectively. At the total frozen condition, *i.e.*, $\omega_u = 0$, the volumetric heat capacity is expressed by C_f, which can be evaluated by Eq. (3) and basic soil properties as listed in Tables 1 and 2. At the total unfrozen condition, *i.e.*, $\omega_f = 0$, the volumetric heat capacity is expressed by C_u, which can also be evaluated by Eq. (3) and basic soil properties as listed in Tables 1 and 2. During ground freezing process, the value of λ or C should be evaluated based on the unfrozen water content (Eqs. (1) and (2)). As mentioned previously, the relationship of unfrozen water content and temperature as suggested by Willams (2001) is used in the analysis.

Moreover, according to the study of Johansen (1975), the thermal conductivity of soil at the total unfrozen condition (before ground freezing) and total frozen condition can be estimated as

$$k_u = k_s^{(1-n)} k_w^n \qquad \text{(before ground freezing)} \tag{4}$$

$$k_f = k_s^{(1-n)} k_i^{n-w_u} k_w^{w_u} \qquad \text{(frozen soil)} \tag{5}$$

where k_s, k_i, and k_w separately represent the thermal conductivity of the soil particle, ice and water, and n is the porosity of soil.

Therefore, the thermal conductivity of the total unfrozen soil (k_u) and that of total frozen soil (k_f) can be obtained by using Eqs. (4) and (5) with the assumptions of w_u at the initial condition (before ground freezing) and $w_u = 0$, respectively. Moreover, we can use Eq. (5) to evaluate the thermal conductivity of the soil at a certain temperature after ground freezing but not yet reaching the total frozen condition, where the value of w_u can be estimated through the relationship of water content and temperature as suggested by Willams (2001).

3.1 Construction Site W1

Figure 10 displays the 2-D finite element mesh for the vertical profile of the vertical tubes, which is capable of representing the middle part of the vertical frozen zone. Table 3 lists the thermal properties of soil used for analysis, which are evaluated from the basic soil properties listed in Table 1. According to the field condition, the initial temperature of the soil is set to be 24°C. The boundary condition for the soil adjacent to air was set to be the convective type of heat transfer. The coefficient of convective heat transfer was obtained through the Nusselt number.

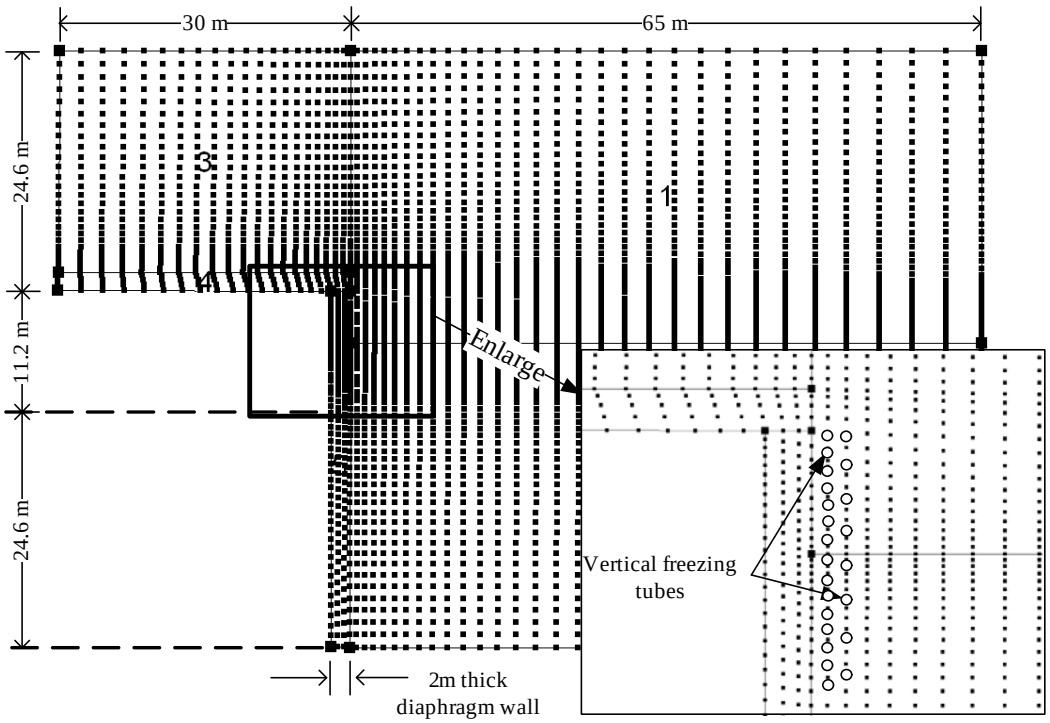

Fig. 10 The 2-D finite element mesh cut across the vertical profile of the treated zone for the construction site W1

Table 3 Thermal properties used in the analysis of the construction site W1

Depth (m)	C_u (kJ/m^3-°C)	C_f (kJ/m^3-°C)	k_u (kJ/m-day-°C)	K_f (kJ/m-day-°C)	w_u (%)
–2.2	2540.57	1883.13	131.34	202.82	35.06
–6	2365.49	1710.87	119.27	200.36	41.86
–17.2	2777.39	1947.48	119.84	200.49	41.52
–23.7	2732.69	1925.41	119.84	200.49	41.52
–28	2755.45	1938.75	120.43	184.92	41.18
–33.6	2650.22	1926.78	128.31	202.22	36.71
–36.2	2524.18	1885.16	133.76	203.29	33.77
–42.5	2765.57	1951.32	122.88	201.12	39.76
–70	2459.07	1793.84	126.88	201.94	37.50

Figure 11 compares the results from the two dimensional finite analysis with those from the field measurements for the sensors at depths of 31.3 m (VTX-05) and 33.3 m (VTX-04). To evaluate the prediction accuracy, the predicted temperatures relative to the monitored ones are depicted and its variances are calculated. Figure 12, along with the variances (R^2 values), is an example for VT5-04 and VT5-05 for such an evaluation. The overall evaluations for the selected sensors are listed in Table 4. As shown in Fig. 11 or Table 4, apart from VT1 and VT2, in which the R^2-values are less than 0.90, the predicted temperatures were generally close to those from the field measurements at the middle part of the frozen region, which virtually subsumed to the two dimensional condition. The reason for the difference existing between the measurements and predicted results may attribute to the complicated boundary condition which was not accurately modeled with the 2D analysis.

Table 4 The variance of predicted and measured temperatures for the construction site W1

Sensors	R^2	Sensors	R^2
VT1-04	0.834	VT1-05	0.838
VT2-04	0.864	VT2-05	0.843
VT3-04	0.969	VT3-05	0.969
VT4-04	0.963	VT4-05	0.958
VT5-04	0.970	VT5-05	0.971

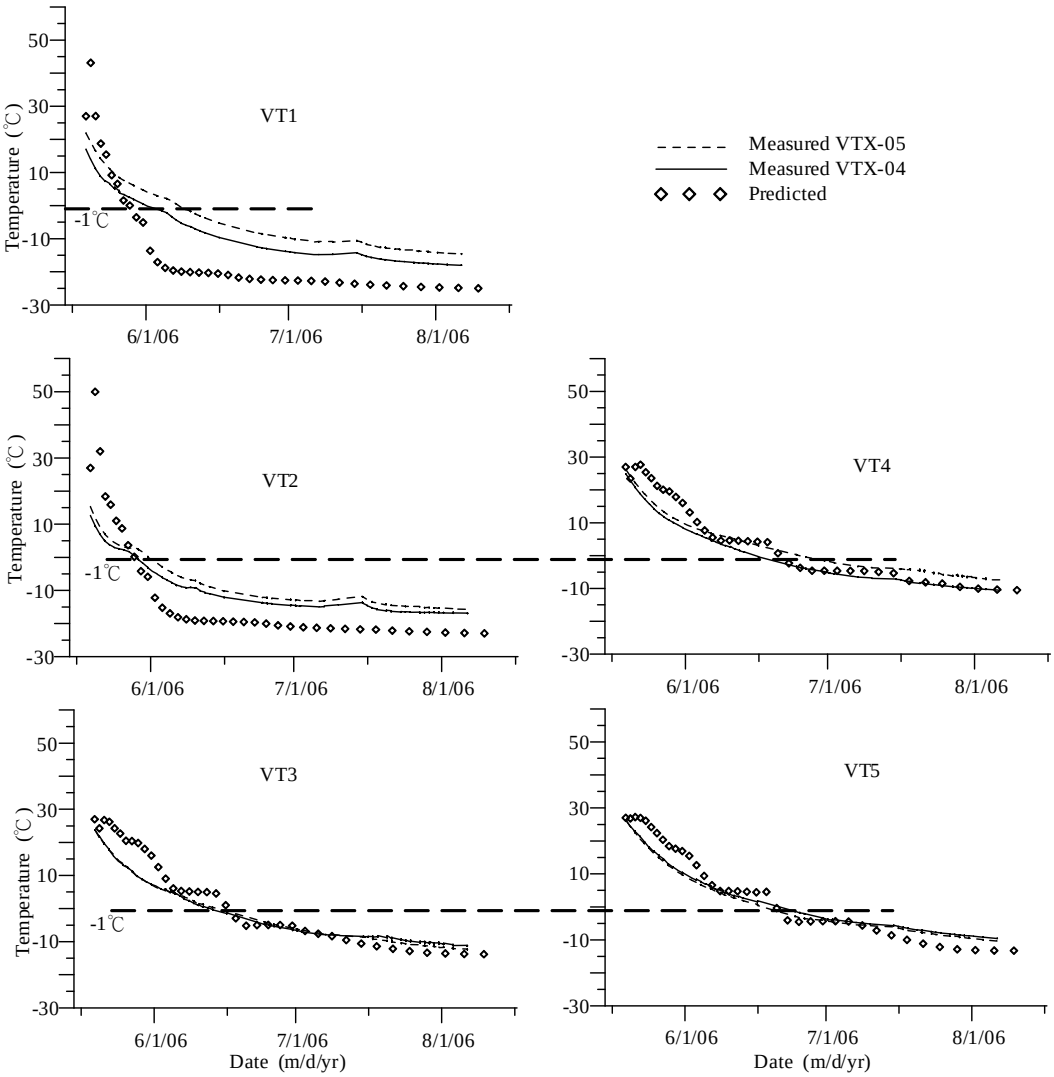

Fig. 11 Comparisons of measured and analyzed temperature changes for the construction site W1

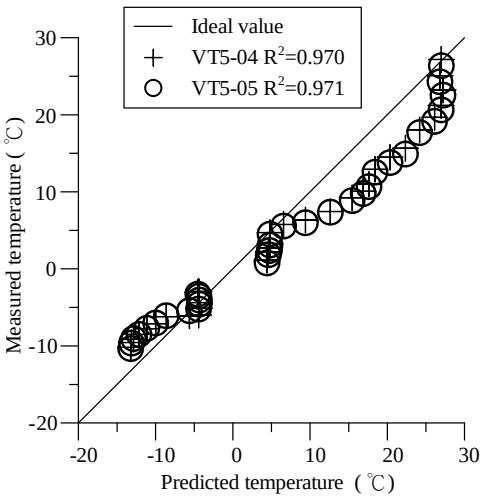

Fig. 12 Relationship of predicted and measured temperatures and their variances for VT5

3.2 Construction Site E

Figure 13 displays the 2D finite element mesh for the horizontal freezing tubes, which is capable of representing the middle part of the frozen zone. Table 5 lists the thermal properties of soil used for analysis, which are evaluated from the basic soil properties listed in Table 2. The temperatures at the location of sensors, 0.6 m from the freezing tubes, predicted from the finite element analysis were compared with those from the field measurements at the middle part of the temperature measurement tubes, such as EAHTX-04, -05, and EAHTX-06. Similar to Fig. 12, the variances for the predicted and measured temperatures are calculated as listed in Table 6. As shown in Fig. 14 or Table 6, the predicted values for EATH4 and EATH5 are lower than those from the field measurements ($R^2 < 0.90$) and otherwise the predicted temperatures were in good agreement with the field measurements. As mentioned previously, the temperature at the measurement tubes of EAHT4 and EAHT5 were higher than that at the other tubes.

It is also found that the predicted temperature of the soil at a distance 0.8 m from the freezing tubes also fell below the frozen point at the 10th of January 2007, that is, the frozen soil would be more than 1.6 m in thickness and more than 4.5 m in length. Therefore, the mirror-face breaking executed at the 16th of January 2007 was appropriate.

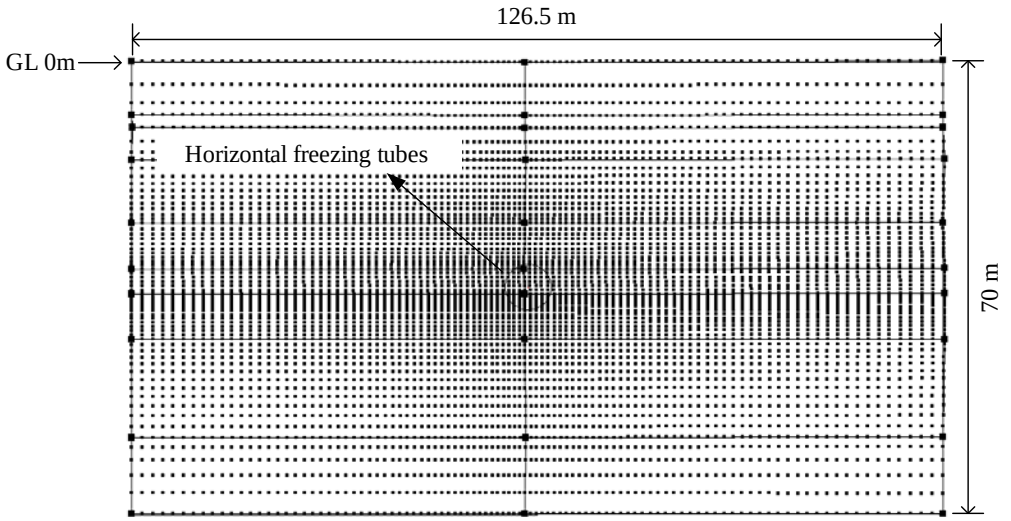

Fig. 13 The 2-D finite element mesh cut across the horizontal freezing tubes for the construction site E

Table 5 Thermal properties used in the analysis of the construction site E

Depth (m)	C_u (kJ/m^3-°C)	C_f (kJ/m^3-°C)	k_u (kJ/m-day-°C)	k_f (kJ/m-day-°C)	w_u (%)
–8	2844.29	1901.45	102.40	196.54	52.61
–10	2385.49	1718.83	123.51	201.25	39.39
–15	3063.62	2048.59	105.15	197.20	50.74
–25	3041.78	2035.62	107.41	197.73	49.24
–32	2860.20	1971.89	117.05	199.89	43.18
–36	2817.72	1967.81	117.23	199.93	43.07
–43	2819.69	1977.14	118.28	200.15	42.45
–58.25	2516.43	1852.15	125.16	201.59	38.46
–70	2707.95	1975.40	126.88	201.94	37.50

Table 6 The variance of predicted and measured temperatures for the construction site E

Sensors	R^2	Sensors	R^2	Sensors	R^2
EAHT1-03	0.905	EAHT1-04	0.915	EAHT1-05	0.946
EAHT2-03	0.959	EAHT2-04	0.964	EAHT2-05	0.950
EAHT3-03	0.880	EAHT3-04	0.873	EAHT3-05	0.890
EAHT4-03	0.876	EAHT4-04	0.849	EAHT4-05	0.702
EAHT5-03	0.908	EAHT5-04	0.908	EAHT5-05	0.885
EAHT6-03	0.801	EAHT6-04	0.898	EAHT6-05	0.908
EAHT7-03	0.794	EAHT7-04	0.948	EAHT7-05	0.949

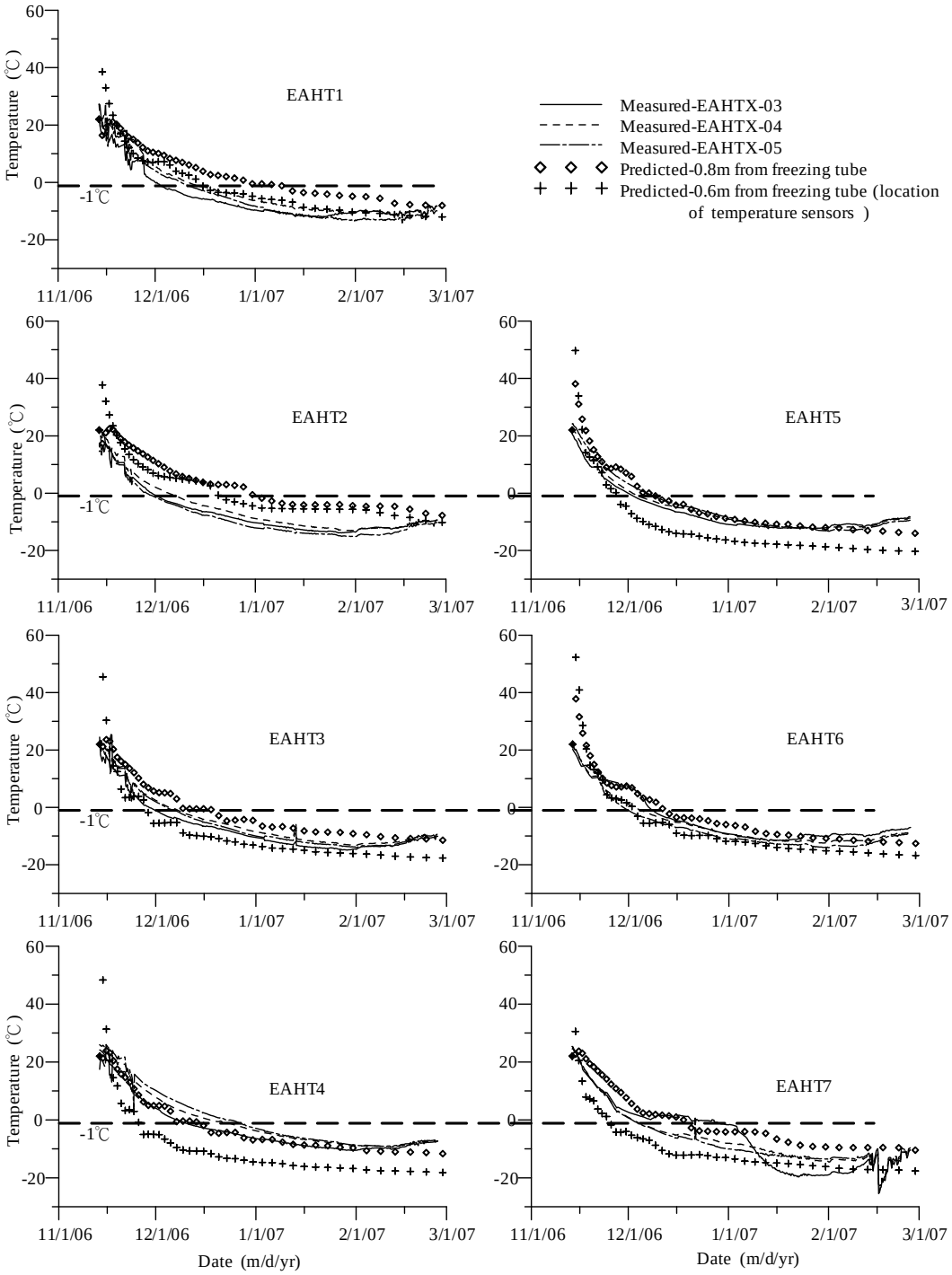

Fig. 14 Comparisons of measured and analyzed temperature changes for the construction site E

4. CONCLUSIONS

With artificial ground freezing in shield tunneling, practical engineers should clearly know how long is required to achieve the minimum thickness of ice wall. It can be done with theoretical analysis, experiences from case studies or numerical analysis. This paper presents the performance of the artificial ground freezing applied in shield tunneling in the construction of the Taipei MRT system. Two case histories at the same site, one with installation of vertical freezing tubes and the other with installation of horizontal freezing tubes, are studied. The temperature of soil at the target region was monitored through the automatic data acquisition system to ensure the range of frozen soil, below –1.0°C. Finite element analysis of temperature change over the period of ground freezing was also carried out, in which the material parameters are determined according to the reasonable procedure described in the paper. Compared with the monitored results, the predicted values were in good agreement with the monitored. The monitored performance of the case histories and numerical analyses certainly facilitates practical engineers in design of artificial ground freezing. Besides, the following conclusion can be drawn:

1. When vertical freezing tubes were installed in two rows with 0.7 m separated each other, one row with 0.8 m in spacing between tubes and the other row with 1.6 m in spacing, frozen confined between GL–27.47 m and GL–39.47 m, it takes 63 days for the soil, 1.8 m thick and 10 m deep, to fall down to the frozen point, −1.0°C. It takes 85 days to reach the frozen region, more than 1.8 m thick and 12 m deep and 147 days to reach the frozen soil, more than 2.0 m thick and more than 12 m deep. For this case history, the temperature of the brine inflowing the freezing tubes were –32°C and temperature flowing out of the tubes were –29.86°C.
2. When 30 horizontal freezing tubes, 6.5 m in length and 3.62 m away from the tunnel center, were uniformly installed around the destined tunnel, with the location of tunnel center at GL–35.5 m and 3.14 m in diameter, it took 54 days for the ring-like of soil, 1.2 m thick and 4.5 m long, to fall down to the frozen point. From numerical simulation, the thickness of the ring-like frozen soil at the 61th day would be more than 1.6 m. For this case history, the temperature of the brine inflowing the freezing tubes were –30°C and temperature flowing out of the tubes were –26.65°C.
3. The temperature of the soil within the frozen zone but near the boundary was slightly less than those at the middle. However, the difference is quite small.
4. The two dimensional finite element analysis with the parameters estimated from the method displayed in this study can be used to predict the temperature of the soil due to artificial ground freezing. Apart from the boundary of the frozen zone, the predicted temperatures were generally close those from the field measurements at the middle part of the frozen region.

ACKNOWLEDGEMENTS

The authors thank the Department of Rapid Transit Systems, Taipei City Government, for providing the authors' chances to do research in the Daocha section and also thank Resources Engineering Services Incorporation for their constructive advices in the analysis of artificial ground freezing.

REFERENCES

Clarke, A. P. J. and MacKenzie, C. N. P. (1994). "Overcoming ground difficulties at Tooting Bec." *Proc. Institute of Civil Engineers*, **102**(2), 60–75.

Crippa, C. and Manassero, V. (2006). "Artificial ground freezing at sophiaspoortunnel (The Netherlands) — Freezing parameters: Data acquisition and processing." *GeoCongress 2006: Geotechnical Engineering in the Information Technology Age*, 254.

Fang, Y. S., Ju, D., Huang, W. C., and Chien, Y. L. (2006). "Rehabilitation of damaged soft ground tunnels." *Journal of GeoEngineering*, **1**(1), 41–49.

Harris, J. S. (1995). *Ground Freezing in Practice*, Thomas Telford, London, U.K.

Huang, C. T., Lin, Y. K., Kao, T. C., and Moh, Z. C. (1987). "Geotechnical engineering mapping of the Taipei city." *Proc. 9th Southeast Asia Geotechnical Conference*, Bangkok, Thailand, **1**, 3-109–3-120.

Johansen, O. (1975). *Thermal Conductivity of Soils*, Ph.D. Dissertation, Trondheim, Norway.

Johnston, G. H., Landanyi, B., Morgenstern, N. R., and Penner, E. (1981). *Engineering Characteristics of Frozen and Thawing Soils*, Edited by Johnston, Permafrost Engineering Design and Constrction, G.H. John Wily and Sons.

Ju, D., Chen, H. T., Sun, L. M., and Duan, S. W. (1997). "Rescue and rehabilitation of a tunnel accident under river." *Proc. Conference on Case Histories of Soft Tunneling*, Chinese Taipei Tunnel Association, Taipei, Taiwan, 91–230.

Krahn, J. (2004), *Thermal Modeling with TEMP/W — An Engineering Methodology*, GEO-SLOPE International Ltd., Canada.

Lackner, R., Amon, A., and Lagger, H. (2005). "Artificial ground freezing of fully saturated soil: Thermal problem." *Journal of Engineering Mechanics*, **131**(2), 211–220.

Lai, Y. M., Zhang, X. F., and Yu, W. B. (2005). "Three-dimensional nonlinear analysis for the coupled problem of the heat transfer of the surrounding rock and the heat convection between the air and the surrounding rock in cold-region tunnel." *Cold Regions Science and Technology*, **20**(4), 323–332.

Li, S., Lai, Y., Zhang, M., and Zhang, S. (2006). "Minimum ground pre-freezing time before excavation of Guangzhou subway tunnel." *Cold Regions Science and Technology*, **46**, 181–191.

Whittaker, B. N. and Frith, R. C. (1990). "Tunneling design, stability and construction." *Institution of Mining and Metallurgy*, England, 219–226.

Woo, S. M. and Moh, Z. C. (1990). "Geotechnical characteristics of soils in Taipei basin." *Proceeding of 10th Southeast Asian Geotechnical Conference, Special Taiwan Session*, Taipei, **2**, 51–65.

Yang, G. R. and Chao, C. L. (1997). "Construction of ventilation shaft for Hsin-tien line lot CH221 of TRTS." *Proc. 7th Conference of Current Researches in Geotechnical Engineering*, 1017–1024.

Yang, P. and Pi, A. R. (2001). "Study on the effects of large groundwater flow velocity on the formation of frozen wall." *Chinese Journal of Geotechnical Engineering*, **23**(2), 167–171.

Yu, Z. K., Huang, H. W., and Wang, R. L. (2005). "Application of the artificially ground freezing method to shanghai metro engineering." *Journal of Glaciology and Geocryology*, **27**(4), 550–556.

Zhou, X. M., Su, L. F., and He, C. J. (1999). "Horizontal ground freezing method applied to tunneling of Beijing underground railway system." *Chinese Journal of Geotechnical Engineering*, **21**(3), 319–322.